Comparative Medicine
Copyright 2024
by the American Association for Laboratory Animal Science

Vol 74, No 1
February 2024
Pages 3–11

Original Research

Binding Affinity, Selectivity, and Pharmacokinetics of the Oxytocin Receptor Antagonist L-368,899 in the Coyote (*Canis latrans*)

Sara M Freeman, PhD,[1,*] J Leon Catrow, PhD,[2,3] James Eric Cox, PhD,[2,3] Alexandra Turano, PhD,[1] McKenna A Rich, BS,[1] Hillary P Ihrig, BS,[1] Naveena Poudyal,[4] Cheng-Wei Tom Chang, PhD,[4] Eric M Gese, PhD,[5,6,7] Julie K Young, PhD,[5,6,7] and Aaron L Olsen, MS, DVM, PhD[8]

L-368,899 is a selective small-molecule oxytocin receptor (OXTR) antagonist originally developed in the 1990s to prevent preterm labor. Although its utility for that purpose was limited, L-368,899 is now one of the most commonly used drugs in animal research for the selective blockade of neural OXTR after peripheral delivery. A growing number of rodent and primate studies have used L-368,899 to evaluate whether certain behaviors are oxytocin dependent. These studies have improved our understanding of oxytocin's function in the brains of rodents and monkeys, but very little work has been done in other mammals, and only a single paper in macaques has provided any evidence that L-368,899 can be detected in the CNS after peripheral delivery. The current study sought to extend those findings in a novel species: coyotes (*Canis latrans*). Coyotes are ubiquitous North American canids that form long-term monogamous pair-bonds. Although monogamy is rare in rodents and primates, all wild canid species studied to date exhibit social monogamy. Coyotes are therefore an excellent model organism for the study of oxytocin and social bonds. Our goal was to determine whether L-368,899 is a viable candidate for future use in behavioral studies in coyotes. We used captive coyotes at the USDA National Wildlife Research Center's Predator Research Facility to evaluate the pharmacokinetics of L-368,899 in blood and CSF during a 90-min time course after intramuscular injection. We then characterized the binding affinity and selectivity of L-368,899 to coyote OXTR and the structurally similar vasopressin 1a receptor. We found that L-368,899 peaked in CSF at 15 to 30 min after intramuscular injection and slowly accumulated in blood. L-368,899 was 40 times more selective for OXTR than vasopressin 1a receptors and bound to the coyote OXTR with an affinity of 12 nM. These features of L-368,899 support its utility in future studies to probe the oxytocin system of coyotes.

Abbreviations and Acronyms: AVP, arginine vasopressin; AVPR1a, vasopressin 1a receptor; LVA, linearized vasopressin antagonist; MRM, multiple reaction monitoring; NWRC, National Wildlife Research Center; OBD, optical binding values; OVTA, ornithine vasotocin analog; OXT, oxytocin; OXTR, oxytocin receptor; PTFE, polytetrafluoroethylene

DOI: 10.30802/AALAS-CM-23-000044

Introduction

Oxytocin (OXT) is a hormone that is produced in the brain and acts at oxytocin receptors (OXTRs) to modulate social behavior in animals and humans. To demonstrate that a hormone like OXT is necessary for a behavior of interest (e.g., pair bonding), studies are needed in which the endogenous receptor system for that hormone is blocked by administration of a selective receptor antagonist—a manipulation that would be expected to subsequently reduce or eliminate the expression of the behavior of interest. A behavioral pharmacology experiment of this design can indicate whether a specific hormone is required for the typical expression of the measured behavior. To this end, several drugs have been developed to specifically target and block OXTR, but most have been developed for peripheral action (e.g., to prevent preterm labor by antagonizing uterine OXTR[42]) or for in vitro experimentation. In recent years, one agent has emerged as the best option to antagonize neural OXTR after peripheral delivery: L-368,899.

The Merck compound L-368,899 is a commercially available, nonpeptide, small-molecule, selective OXTR antagonist that was originally developed as a drug to prevent preterm labor in humans.[27,45] Although its utility was limited for that goal because of suboptimal oral bioavailability and pharmacokinetics in primates,[13,42] the compound has been used for many decades for neuroscience research in animals to block OXTR in the brain after peripheral administration, which allows assessment of the involvement of the OXT system in social behavior. L-368,899 has been reported to accumulate in the rhesus monkey brain after peripheral administration[2] and to affect social behavior in rhesus monkeys,[2] marmoset monkeys,[5-8,20,24,35,39] lambs,[25] and a growing number of studies in rodents.[3,11,14,15,17,23,36-38,41,43,44]

Submitted: 11 Jul 2023. Revision requested: 18 Oct 2023. Accepted: 27 Jan 2024.
[1]Department of Biology, Utah State University, Logan, Utah; [2]Metabolomics, Proteomics, and Mass Spectrometry Cores, University of Utah, Salt Lake City, Utah; [3]Department of Biochemistry, University of Utah, Salt Lake City, Utah; [4]Department of Chemistry & Biochemistry, Utah State University, Logan, Utah; [5]Department of Wildland Resources, Utah State University, Logan, Utah; [6]Ecology Center, Utah State University, Logan, Utah; [7]US Department of Agriculture, Wildlife Services, National Wildlife Research Center, Predator Research Facility, Millville, Utah; and [8]Animal Dairy and Veterinary Sciences Department, Utah State University, Logan, Utah
**Corresponding author. Email: sara.freeman@usu.edu*

Behavioral pharmacology studies in nonhuman animals have been crucial to our understanding of the neurophysiology of OXT, but they have all relied on a single publication reporting that L-368,899 penetrates the blood brain barrier and accumulates in the CNS after peripheral injection.[2] Although a strength of this study was that it quantified L-368,899 in CSF at seven time points after injection over a time period of nearly 4 h, the study had some limitations. For example, only two CSF sampling time points were collected per subject across only four subjects, and the time points were all different across the four subjects. This design resulted in two notable limitations. First, each time point had a sample size of one, making it impossible to evaluate variability across subjects. Second, a single sample from one subject served as the baseline for the entire study. Thus, although the study did report detectable levels of L-368,899 in CSF across subjects across time, the data do not allow general conclusions about the pharmacokinetic profile of L-368,899 in the CNS. The study also used postmortem brain specimens collected 60 min after an intravenous infusion of 1 mg/kg L-368,899 and subdissected eleven brain regions (two to four specimens per region) for quantification of L-368,899. The data provide the only evidence that L-368,899 can be detected in the brain and CSF after intravenous administration, but the entire field of OXT research relies on this compound to centrally manipulate behavior in many different species and after a variety of different doses and routes of administration; therefore, the findings of the previous publication[2] may not be generalizable across species, routes of administration, doses, or time courses.

The current study seeks to extend the findings of that single paper in a novel species—coyotes (*Canis latrans*). OXT is involved in social bonding in monogamous rodents and monkeys,[12] but little work has been done in monogamous mammals outside of those groups. Coyotes form lasting pair bonds as a feature of their monogamous mating structure.[16,22] In fact, Canidae is one class of highly social mammals that has been insufficiently studied with respect to the biologic basis of social attachment. Although monogamy is relatively rare in mammals (3 to 9% of mammals; 16% of carnivores; 15 to 25% of primates),[10,18,19,21,22,26] all wild canid species studied to date exhibit social monogamy. In no other group of mammals is pair bonding this prevalent.[22] This feature of canids renders them particularly suitable for the biologic study of social attachment. We aimed to determine whether L-368,899 is a viable candidate for future use in in vivo behavioral studies in coyotes that will test whether various canid social behaviors are OXT dependent. These behavioral pharmacology studies using selective, brain-penetrant antagonists are critical to our overall understanding of the neurophysiology of OXT in canids more broadly and can help to determine whether the mechanisms driving mammalian pair-bonding are shared or unique across taxa.

To assess the potential use of L-368,899 for future behavioral experiments in coyotes, we performed two studies. The first was a terminal study conducted in vivo to assess the pharmacokinetics of peripherally administered L-368,899 in adult coyotes. This study evaluated the time course of L-368,899 in blood and CSF using paired sampling over a 90-min period, and it then attempted to confirm the presence or absence of the drug in eight subregions of the coyote brain. We expected to see a significant increase in L-368,899 in blood and CSF in all samples as compared with baseline, with a peak in blood and CSF between 15 and 45 min after administration. Our second experiment was conducted in vitro using coyote brain tissue sections to determine the binding affinity and selectivity of L-368,899 for coyote OXTR and the structurally similar vasopressin 1a receptor (AVPR1a). We sought to validate that L-368,899 binds selectively to OXTR with high affinity in the coyote brain. Together, these studies provide foundational information on the pharmacokinetic profile and binding selectivity of this drug in a novel mammal and model organism to advance the study of canid social behavior.

Methods

Experiment 1: pharmacokinetics of peripherally administered L-368,899 in the coyote. ***Drug information.*** L-368,899 is commercially available from Tocris (Minneapolis, MN) and was formulated in saline to 3 mg/kg for intramuscular injection. In male marmosets, this dose given intramuscularly blocked the OXT-induced increase in time spent looking at the eye region of photo of a conspecific[20]; in a female macaque, this dose given intravenously reduced interest in an infant and impaired sexual behavior.[2] Intranasal administration has commonly been used in research targeting the OXT system in vivo, but this delivery method is not feasible with coyotes in this facility for a number of logistical and scientific reasons. First, the facility manages and cares for coyotes using husbandry methods that maintain wild behavior[29]; therefore, it was not desirable to perform the extensive habituation and training would be required for subjects to tolerate restraint for precise intranasal delivery. Second, the (repeated) restraint required for intranasal administration would cause considerable stress to the animal and increase the risk of physical harm to the experimenter. Third, one of the primary advantages of intranasal drug delivery—increased penetration into the CNS as compared with systemic routes—is not as important for this small-molecule antagonist, as it is for the administration of OXT (a peptide) itself. L-368,899 is a nonpeptide compound with molecular features that promote its ability to cross the blood-brain barrier (e.g., lipophilic, low molecular weight), and it has been shown to have central effects on behavior when administered intramuscularly to common marmosets (*Callithrix jacchus*).[20] Above all, the purpose of the study was to evaluate the use of this drug for future behavioral pharmacology studies in coyotes. Therefore, we wanted to use a route of administration that would 1) minimize stress to the subject before release into a behavioral testing paradigm and 2) be easily incorporated into the routine capture and handling protocols that the animals and staff are already accustomed to. Intramuscular injections are quick, are routinely administered by the staff at the coyote facility,[4] and, in contrast to oral administration, ensure that the entire dose is delivered in a short time frame. Even though L-368,899 has good oral availability in rats and dogs[40] and has been given orally to marmoset monkeys in a palatable food item before behavioral testing,[5-8,24,35,39] intramuscular injections provide a more controlled route of administration for delivery of an exact, bolus dose without any issues of variability in the amount of food consumed. Furthermore, intramuscular injections also bypass the first-pass metabolism of the drug and eliminate any variability from gastric factors on drug absorption.

Animals. All subjects were housed at the USDA National Wildlife Research Center (NWRC) Predator Research Facility, which maintains a colony of captive coyotes for research purposes. Approximately 90 to 100 adult male and female coyotes are housed as pair-mates in outdoor enclosures (0.001 to 0.01 km^2) that are surrounded by chain-link fencing and contain at least one manmade den box, two shade tables, and an ad libitum source of water. Each coyote was fed approximately 650 g of a high-protein, high-fat, meat-based mixture (Fur Breeders Agricultural Cooperative, Logan, UT) at least 6 d per week, and

enrichment items were provided whenever possible. Animal care staff completed health and welfare checks on each coyote daily. The five adult coyotes (two males; three females) that were used in this study were slated for euthanasia based on colony-management decisions related to animal age. All subjects were otherwise healthy and had not been exposed to any pharmaceutical compounds over their lifetime beyond those used in routine veterinary care (e.g., vaccines, heartworm preventative) or the occasional immobilization drugs (only if needed). The only previous studies in which these subjects could have participated would have been behavioral experiments related to coyote sociality or the reduction of human-coyote conflicts. Our euthanasia protocol (SOP AC/UT 002.01) includes sedating coyotes with a combination of ketamine hydrochloride and xylazine hydrochloride before administering a lethal injection of veterinary euthanasia solution (50 mg/mL phenytoin sodium, 390 mg/mL pentobarbital sodium) dosed at 2.2 mL/kg body weight. This study took place after sedation and before the scheduled euthanasia. All procedures were approved by the USDA/NWRC Institutional Animal Care and Use Committee (QA-3357). Males weighed 17.4 and 18.5 kg, and females weighed 14.4, 15.8, and 16.1 kg. Subjects were 9 to 10 y old.

Procedure. All of the following steps took place between approximately 0900 and 1300 on scheduled study days; one or two animals were processed on each study day. Each coyote was captured in a familiar den box in their enclosure, moved in that den box to a procedure room, and sedated with inhaled isoflurane gas (1 to 5% of inhaled oxygen) using a custom den-box cover.[1] After the initial sedation, the animal was placed on an examination table, and an endotracheal tube was placed for delivery of anesthetic and oxygen. Subjects were then maintained on inhaled isoflurane (1 to 5% of inhaled oxygen), and vital signs (body temperature, pulse, and respiration rate) were monitored and recorded every 10 min throughout the procedure. After appropriate analgesia depth was confirmed, a catheter was placed in the cephalic vein of a forelimb to enable repeated blood sampling. To enable repeated CSF collection over time and to minimize the number of separate spinal punctures required, an intrathecal port was placed into the cisterna magna by an experienced veterinarian. The port was closed between sampling time points. After these preparatory steps were completed, baseline blood and CSF samples were taken (t0). The animal then received an intramuscular injection of L-368,899 (3 mg/kg in 1 mL saline, pH 5.5) into the biceps femoris muscle of the hindlimb, and the time of injection was recorded. A time course of paired blood and CSF samples was taken at 15, 30, 45, 60, and 90 min after injection (t15, t30, t45, t60, t90). All blood samples were immediately centrifuged at 4 °C for 15 min; plasma was carefully removed, frozen in 1-mL aliquots, and stored at −80 °C until analysis. CSF samples (1 mL) were immediately placed at −20 °C and then transferred to −80 °C storage until analysis. After 90 min, the animals were euthanized according to approved veterinary practices and NWRC protocols (described above). One subject was excluded from the study because of visible blood contamination of the t15 CSF sample; this subject was euthanized and samples were not contributed to the study, although the untreated baseline CSF and plasma samples were used as blanks to optimize the chemical analysis. We were not able to collect clean CSF samples from one additional subject from t45 onward and only collected t0, t15, and t30 samples for that animal. All other samples were collected as planned without issue.

After death, each subject was transported on ice to the Utah Veterinary Diagnostics Laboratory for brain removal by a veterinary pathologist. Brains were removed within 1 to 3 h after death and rinsed with saline. Eight specific regions of the brain (hippocampus, olfactory bulb, lateral septum, striatum, piriform cortex, straight gyrus, rhinal cortex, and white matter) were then subdissected from the left hemisphere and immediately frozen on dry ice. These eight regions fell into three categories according to ongoing ex vivo receptor autoradiography work in coyote brain sections (Freeman et al., 2024, Utah State University, unpublished): 1) regions known to contain OXTR binding: hippocampus, olfactory bulb, piriform cortex, 2) regions known to contain AVPR1a binding: lateral septum, straight gyrus, rhinal cortex, and 3) control regions that show neither OXTR nor AVPR1a binding: striatum, white matter (corpus callosum). All brain samples were weighed (Table 1) and then stored at −80 °C until analysis.

Sample analysis. All biologic samples were analyzed by liquid chromatography followed by tandem mass spectrometry (LC-MS/MS) in partnership with the Metabolomics, Proteomics, and Mass Spectrometry Cores at the University of Utah to quantify the amount of L-368,899 present in all samples. L-368,899 was derivatized with a trifluoroacetyl group for use as an internal standard.

Plasma and CSF sample extraction. A standard curve of 1,818 ng/mL to 0.02 ng/mL of L-368,899 calibrant solutions was prepared in untreated *C. latrans* CSF or plasma as appropriate. A t0 control containing only untreated (t0) CSF or plasma was used in the calibration curve preparation, and a process blank containing only 10 µL of water was prepared at this time and carried through the extraction. Ten microliters of each calibrant solution was extracted by the addition of ice-cold acetonitrile plus 0.1% formic acid and 0.2 µg/mL internal standard. Extracted samples and calibrants were vortexed for 30 s and then chilled at −20 °C for 1 h. Samples and calibrants were centrifuged for 4 min at 20,000 × *g* and 4 °C. The supernatant was then transferred to polytetrafluoroethylene (PTFE) autosampler vials for analysis.

Brain sample extraction. Brain tissue samples were homogenized in a 5:1 volume:weight ice-cold 80% acetonitrile + 0.1% formic acid extraction solvent in ceramic bead mill tubes for 30 s. A process blank was prepared containing only extraction solvent. Samples were chilled for 1 h at −20 °C. After 1 h, samples were centrifuged for 10 min at 20,000 × *g* at 4 °C. The supernatant was transferred to a new 1.7-mL microfuge tube and transferred to PTFE autosampler vials for analysis.

LC-MS/MS. Plasma and CSF were analyzed using a SCIEX 6500 QTRAP coupled to a SCIEX Nexera Ultra-performance liquid chromatography (UPLC; SCIEX, Framingham, MA). Separation was achieved on an Agilent ZORBAX StableBond 300 C8 2.1 × 100 mm UPLC column (Agilent Technologies, Santa Clara, CA) with ddH_2O + 0.1% formic acid (buffer A) and distilled 95%

Table 1. Weights of subdissected brain region specimens across subjects

Brain region (n = 4)	Mean weight (g) ± SD
Hippocampus	0.720 ± 0.081
Lateral septum	0.184 ± 0.078
Olfactory bulb	0.997 ± 0.254
Piriform cortex	0.263 ± 0.079
Rhinal cortex	0.232 ± 0.057
Straight gyrus	0.611 ± 0.210
Striatum	0.748 ± 0.338
White matter	0.558 ± 0.258

acetonitrile in ddH_2O + 0.1% formic acid (buffer B) as eluents. A flow rate of 0.4 mL/min was used with starting conditions of 1% buffer B and a column temperature of 35 °C. Buffer B was held at 1% for 0.5 min then increased to 85% over 7.5 min. Buffer B was then reduced to 1%, and the column was equilibrated for 5 min between runs. Source conditions and multiple reaction monitoring (MRM) settings for L-368,899 were optimized by SCIEX Analyst: curtain gas, 20 L/min; collision gas, 12 L/min; ion spray voltage, 5,000 V; temperature, 350 °C; ion source gas 1, 50 L/min; ion source gas 2, 60 L/min. Analysis of the brain tissue was conducted on a SCIEX 7600 Zeno-ToF coupled to an Agilent 1290 Infinity II UPLC system (Agilent, Santa Clara, CA). Separation was achieved using a Phenomonex Luna C8 150 × 2.1−mm column (Phenomenex, Torrance, CA). The same eluents, column temperature, and flow rate as the plasma and CSF were used. A gradient method of 1% Buffer B was held for 15 min and then increased to 90% B over 5 min before being returned to starting conditions. The transitions shown in Table 2 were monitored by MRM (SCIEX 6500) or MRM HR with the Zeno trap on (SCIEX 7600), and data were analyzed by SCIEX MultiQuant software and Microsoft Excel.

Statistics. Because of the low sample sizes for CSF (n = 2 to 3) and plasma (n = 4), we used a descriptive approach and display our results in two ways: graphs showing all data points (Figure 1, right panels) alongside graphs showing the means and standard error of the mean (Figure 1, left panels). The brain results were analyzed using a one sample t test and Wilcoxon test to compare the mean levels of L-368,899 in each region of interest to a theoretical mean of 4.620, which was the average value measured in untreated brain tissue. We also pooled all data points across our three categories (control regions, OXTR regions, and AVPR1a regions) and used an ordinary one-way ANOVA to assess whether L-368,899 levels were significantly greater than controls in the OXTR- or AVPR1a-enriched regions of the brain. For all tests, α was set at $P = 0.05$.

Experiment 2: Binding affinity and selectivity of L-368,899 for coyote OXTR and AVPR1a. ***Specimens and tissue processing.*** Because no coyote-specific cell lines or coyote *OXTR* or *AVPR1a* gene plasmids are available for in vitro pharmacology assays using cell culture, we used unfixed cryosections of coyote brain tissue as our source of OXTR and AVPR1a for our in vitro investigation of the binding affinity and selectivity of L-368,899 for coyote OXTR and AVPR1a. Brains for this study came from five additional adult coyotes (two male, three female) that were otherwise healthy and were also housed at the NWRC Predator Research Facility. Husbandry and euthanasia procedures were the same as described above. Specimens were opportunistically acquired based on previously determined euthanasia decisions based on unrelated veterinary or colony-management needs. Brains were removed by a veterinary pathologist within 1 to 3 h after death, rinsed with saline, and blocked into ten coronal hemispheres (five coronal blocks, which were separated along the midline to yield 10 coronal hemispheres). These tissue blocks were immediately frozen flat on a piece of parafilm on a slab of dry ice. Once frozen completely, each block was wrapped in a labeled piece of aluminum foil and stored at −80 °C until sectioning. Blocks were brought up to −15 °C and sectioned into 12 adjacent series at 20 µm thickness on a cryostat. Sections were thaw-mounted on 38 × 75 mm SuperFrost Plus microscope slides, which were then stored at −80 °C in a sealed slide box containing a desiccant packet until use in competitive binding receptor autoradiography.

Competition binding assay. Competitive binding receptor autoradiography was used to determine the binding affinity and selectivity of L-368,899 to coyote OXTR and AVPR1a. Sections of the coyote brain containing regions that were previously determined to contain OXTR or AVPR1a binding sites (Freeman et al., 2024, Utah State University, unpublished observations) were selected for the study (regions of the olfactory pathway for OXTR, namely, the olfactory bulb, olfactory tubercle, and piriform cortex, and the lateral septum for AVPR1a). L-368,899 was initially dissolved from lyophilized powder in dimethyl sulfoxide (DMSO) to 10 mM (max solubility in DMSO is 100 mM). We used this stock solution to create a serial dilution yielding nine logarithmic molarities of L-368,899 in DMSO, ranging from 10 mM (10^{-2}) to 0.1 nM (10^{-10}). When added to the binding assay in a 1:1,000 dilution, these nine working stocks yielded a logarithmic set of nine final molarities of 10 µM (10^{-5}) to 0.1 pM (10^{-13}), encompassing the physiologic range of ligand action at endogenous receptors. Competitive binding receptor autoradiography was carried out as previously described.[31] The sealed boxes were removed from −80 °C storage and allowed to thaw for 1 h at room temperature. Then, the slides were briefly fixed in 0.1% paraformaldehyde in PBS (pH 7.4) and rinsed twice in 50 mM Tris buffer (pH 7.4). Slides were then coincubated for 1 h in 50 pM of the OXTR radioligand, ^{125}I-ornithine vasotocin analog (^{125}I-OVTA; PerkinElmer), or the AVPR1a radioligand ^{125}I-linearized vasopressin antagonist (^{125}I-LVA; PerkinElmer) with one of nine different increasing concentrations of L-368,899, as described above. After this incubation, unbound radioligand was removed by two 10-min washes in 50 mM Tris buffer plus 2% $MgCl_2$ (pH 7.4) and then dipped into ddH2O and allowed to air dry. Once dry, the slides were exposed in complete darkness to BioMax XAR film (Carestream) for 5 d with a set of 10 ^{125}I standards (American Radiolabeled Chemicals).

Quantification. Film was developed in a darkroom and analyzed as follows using MCID Core Digital Densitometry software and associated top-mounted camera and light box. After determining a flat field correction for luminosity across the field of view, optical binding density (OBD) values from the set of standards were loaded into the software and used to generate a standard curve. For OXTR quantification, boundaries were drawn around regions of dense OXTR radioligand binding in the olfactory pathway, which had no appreciable AVPR1a binding (e.g., piriform cortex, the olfactory tubercle); for AVPR1a, one region of dense AVPR1a radioligand binding that did not have OXTR signal (e.g., lateral septum) was quantified. The region quantified was consistent across all concentrations for each specimen. An average OBD measurement was calculated

Table 2. MRM transitions

Precursor (Da)	Product (Da)	Compound	DP (V)	EP (V)	CE (V)	CXP (V)
555.267	136.0	L-368,899	10	13	35	14
555.267	177.2	L-368,899	80	13	35	12
555.267	244.1	L-368,899	80	11	35	12
651.0	152.0	Internal standard	10	13	35	14

CE, collision energy; CXP, collision cell exit; DP, declustering potential; EP, entrance potential; V, volts.

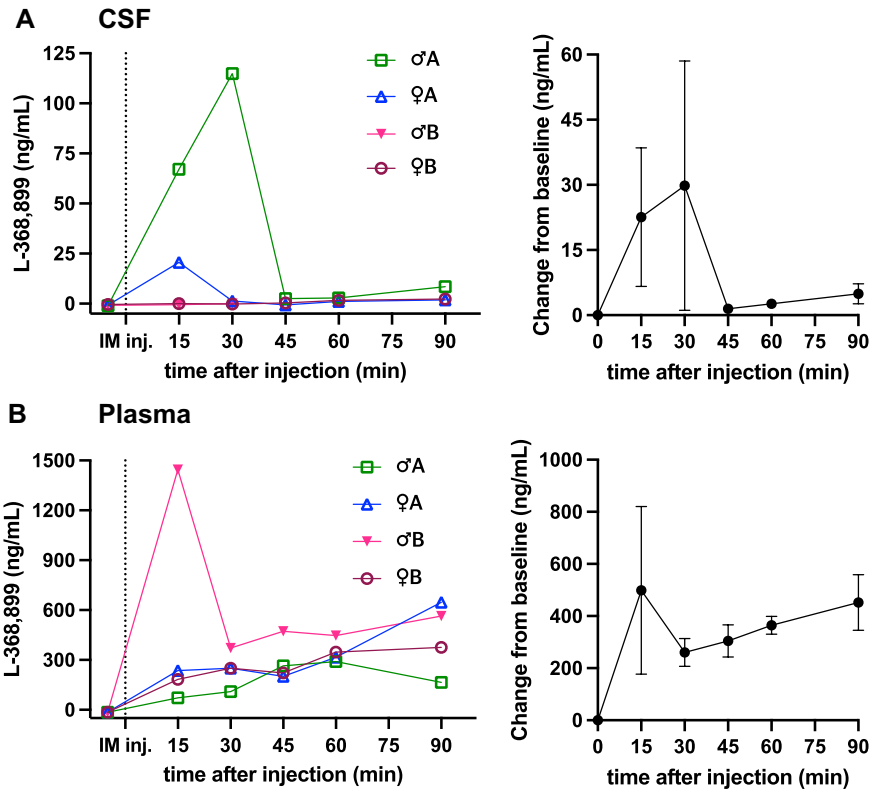

Figure 1. Pharmacokinetics of L-369,899 in coyote CSF (A) and plasma (B). For each panel, graphs on the right show the mean ± SEM for the raw data displayed on the left.

at each concentration of L-368,899, and these values were used to calculate a proportion of maximum radioligand binding across all concentrations relative to the 10^{-12} or 10^{-13} competitor condition. GraphPad Prism was used to calculate the binding affinity (K_i) of L-368,899 to OXTR and to AVPR1a and to generate competition curves (one-site fit K_i) for each.

Results

Experiment 1: Pharmacokinetics of peripherally administered L-368,899 in the coyote. ***CSF.*** Of the four subjects, one female showed no change in detectable L-368,899 at any of the postinjection time points as compared with t0. The male from which we obtained only 3 CSF samples (t0, t15, and t30) also showed no change. In the remaining two subjects, the CSF levels of L-368,899 peaked at t15 for the female and at a much higher level at t30 for the male (Figure 1A). The levels of L-368,899 in these two subjects had returned to baseline by t45.

Plasma. We successfully obtained plasma samples at all time points for all four subjects. One subject showed a marked increase in detected L-368,899 at t15, but, across subjects, levels of L-368,899 in plasma increased gradually over time, consistent with muscular absorption (Figure 1B). Overall, levels of measured L-368,899 per milliter of plasma were more than 10-fold higher than levels measured in CSF, as would be expected after intramuscular administration.

Brain. Because of unexpected issues with the internal standard, we were unable to quantify absolute levels of L-368,899 in our brain samples. Specifically, it appeared that a small amount of underivatized parent compound (L-368,899) was present in the internal standard, indicating issues with purity, which caused some small amounts of our target drug to be measured in our untreated control samples. However, we were able to generate relative values across brain regions, which can be compared with one another and to baseline levels in untreated brain samples. The values reported are the AUC divided by the weight (mg) of brain tissue used in the assay. Qualitatively, L-368,899 is clearly present above background levels in a majority of our regions of interest (Figure 2), especially lateral septum, rhinal gyrus, piriform cortex, and hippocampus, but none of the regions were statistically different from the average AUC/mg of untreated brain tissue (dotted line, Figure 2). When all data points were pooled for each category of brain area, neither OXTR-enriched brain samples nor AVPR1a-enriched brain samples were significantly different from controls ($P = 0.467$ and $P = 0.094$, respectively).

Experiment 2: Binding affinity and selectivity of L-368,899 for coyote OXTR and AVPR1a. L-368,899 bound to the coyote OXTR with an affinity of K_i =12.38 nM, whereas its affinity for the coyote AVPR1a was more than 40-fold lower, at K_i =511.6 nM (Figure 3).

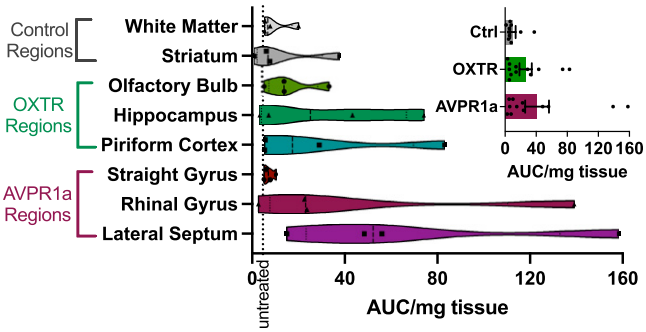

Figure 2. Relative abundance of L-368,899 in 8 subregions of the coyote brain after peripheral injection. Values are reported as AUC per weight (mg) of analyzed tissue. The dotted line is the average of 2 control samples (brain tissue from a subject that did not receive any drug injection) (4.62 = (4.72 + 4.51) / 2). The inset graph shows average data for the 3 brain region categories.

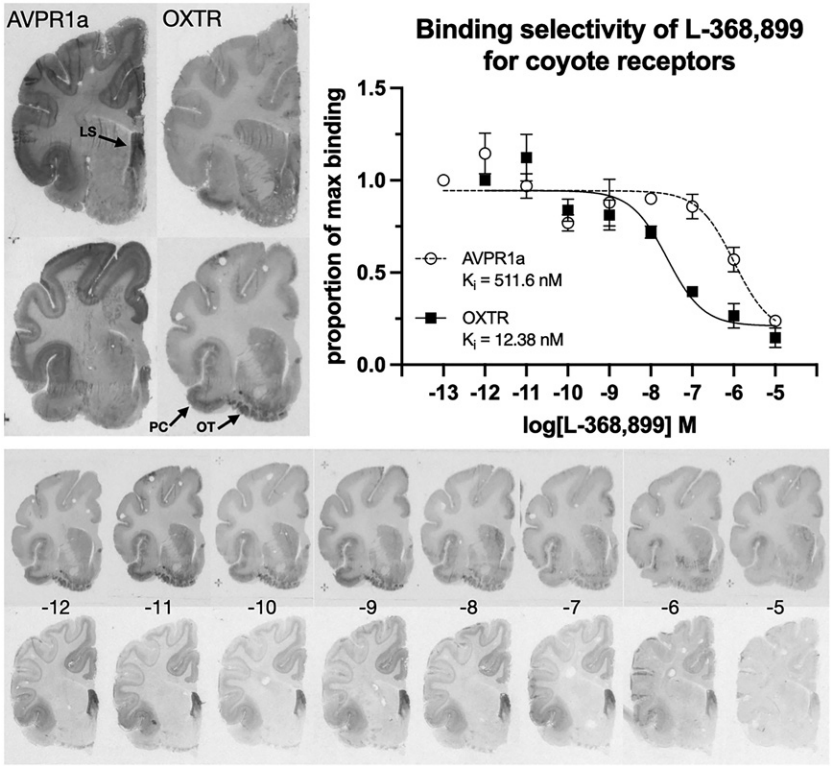

Figure 3. Binding selectivity of L-368,899 for coyote OXTR and AVPR1a in brain. Top left: left 2 images show representative autoradiograms of AVPR1a binding; right images show corresponding OXTR binding in an adjacent section from the same brain; brain regions that were quantified for specific binding of each receptor subtype are indicated by arrows: AVPR1a in lateral septum (LS) and OXTR in regions of the olfactory pathway, specifically piriform cortex (PC) or olfactory tubercle (OT). Top right: curves showing binding selectivity of L-368,899 in the coyote brain; each point represents the mean ± SEM for 5 independent measures of receptor binding density. For the OXTR competition curve, all values are represented as a proportion of maximum binding of the ^{125}I-OVTA radioligand in the presence of 10^{-12} M (1 pM) of L-368,899. For the AVPR1a competition curve, all values are represented as a proportion of maximum binding of the ^{125}I-LVA radioligand in the presence of 10^{-13} M (0.1 pM) of L-368,899. Bottom: representative series of competition binding results showing OXTR binding (top row) and AVPR1a binding (lower row) in the presence of the log[L-368,899] M indicated (−12 to −5).

These results indicate that L-368,899 is highly selective for the coyote OXTR, especially at a concentration of 10^{-7} M, or 10 nM.

Discussion

This study provides the first pharmacological assessments of the OXTR antagonist L-368,899 in the coyote. We found that L-368,899 peaked in the CNS at t15 or t30 after intramuscular injection and returned to baseline by t45. This pharmacokinetic profile, although based on a limited number of subjects, suggests that the best window for behavioral testing would be 15 to 45 min after injection when using intramuscular delivery of 3 mg/kg L-368,899. Aside from a single animal with a peak at t15 in plasma, we found a generally slow plasma absorption profile, with continuously increasing levels of drug in the bloodstream throughout the entire 90-min time course of our study. This result indicates that L-368,899 remains in circulation much longer than it remains in CSF. In the context of a behavioral pharmacology study, these data suggest that, if behavioral testing were to continue longer than 45 min, changes in behavior could not be attributed solely to central effects of L-368,899 at these later time points because of the potential for drug action at peripheral OXTR.

Although our brain analysis did not yield absolute values of quantified µg of L-368,899 per mg of brain tissue, we were able to measure relative levels of L-368,899 across regions across all four subjects, and two of our four subjects exhibited peaks of L-368,899 in CSF. The individual subject with the highest peak in CSF levels of L-368,899 was also the individual with the highest levels of detected L-368,899 in the piriform cortex and olfactory bulb—two of the most OXTR-enriched regions of the coyote brain, based on ongoing work from our lab. Unexpectedly, two of the regions with the highest relative levels of L-368,899—the lateral septum and rhinal cortex—are both AVPR1a-expressing areas based on receptor autoradiography results from our lab. Although L-368,899 may be high in the lateral septum and rhinal cortex because it is binding to AVPR1a, our in vitro binding selectivity data suggest that L-368,899 has a high specificity for the coyote OXTR and exhibits a 40-fold greater affinity for OXTR than for AVPR1a. Despite this selective binding profile, L-368,899 could still bind to AVPR1a in vivo if the local concentration achieved in certain brain areas is near or greater than the drug's affinity for AVPR1a (approximately 500 nM). This unexpected result may be driven by the data from one individual subject that had the highest drug levels measured in both of these areas, although that same subject had no detectable drug in CSF across the full 90-min time course. Individual differences in the rate of brain penetration from CSF or differences in the retention or clearance of drug from neural receptors could also cause discrepancies between the levels of drug measured in CSF and the levels in the brain at necropsy. We were careful to euthanize all subjects immediately after the 90-min collection time point, and all brains were removed and frozen within 1 to 3 h of euthanasia. However, the appropriate research tools are not available to allow assessment of these details of in vivo receptor occupancy; assessing these nuanced in vivo kinetics of neural receptor binding would require an OXTR or AVPR1a tracer for in vivo PET neuroimaging, neither of which are available despite extensive

Table 3. Comparison of the binding affinities and selectivity of L-368,899 to OXTR and AVPR1a across mammalian species that have been evaluated to date

Species	Binding affinity OXTR (nM)	Binding affinity AVPR1a (nM)	Binding selectivity (AVPR1a K_i ÷ OXTR K_i)
Rat[27]	3.6 ± 0.5 (uterus); 8.9 ± 0.5 (mammary)	110 ± 13 (liver)	12.4 – 30.6
Macaque[28]	20 ± 1 (uterus)	170 ± 30 (liver)	8.5
Human[27]	13 ± 1 (uterus); 7.6 ± 1.8 (cloned)	180 ± 23 (liver)	13.8 – 23.7
Coyote	12.4 ± 3.4 (brain)	512 ± 117 (brain)	41.2

efforts (including studies using L-368,899 as a potential parent compound for a ^{18}F radiotracer).[30-34] More precise analytical chemistry will be required to confirm the amount of drug present regionally in the brain after peripheral injection, especially with regard to the internal standard and extraction method.

Besides our methodological issues with quantification of L-368,899 in brain samples, another caveat with our brain analysis is that all samples were taken at the end of the 90-min time course, well after all CSF samples had returned to baseline. This experimental design decision reduced the number of animals needed for a terminal study but added difficulty to the interpretation that a lack of detected L-368,899 in the brain means a lack of action of L-368,899 at neural receptors. As in CSF, the drug may not be detectable in brain tissue that long after drug delivery. Future studies to evaluate the presence of L-368,899 in coyote brain should perform euthanasia 30 min after drug administration to coincide with the peak levels of drug in CSF.

Rapid or variable liver metabolism could also have contributed to our results. At least two previous publications have described rather extensive first-pass liver metabolism of orally and intravenously administered L-368,899 at a variety of doses, especially in rhesus macaques, but less drastically so in rats, dogs, and chimpanzees.[9,40] The main breakdown product of L-368,899 is methionine sulfone, which to our knowledge, is not pharmacologically active at OXTR. Sex differences in the rate of hepatic breakdown of L-368,899 have been reported in rats, but only at high doses (10, 25, and 100 mg/kg).[40] Although coyotes may show rapid liver metabolism of this compound like that described in rhesus macaques, we assume that hepatic function and breakdown rates of coyotes would be similar to what has been described for this compound in dog, which was relatively slow and stable. Future studies should directly address sex differences, which our study was not sufficiently powered to allow. Furthermore, doses higher than 3 mg/kg may be needed in coyotes and/or for intramuscular delivery to achieve biologically active concentrations of L-368,899 in brain; we acknowledge that one limitation of our study was the use of only one drug dose.

Compared with the plasma and CSF levels of L-368,899 measured in the previous study in primates,[2] our values mostly align, but we detected much higher peak values. Specifically, our highest levels of L-368,899 measured in CSF ranged from 20 to 115 ng/mL, with the majority of values around 0.5 to 8 ng/mL, whereas all CSF values from the previous report[2] ranged between 0 and 10 ng/mL. In plasma, our levels ranged from 0 to 700 ng/mL with a peak at 1,450 ng/mL, whereas levels in the previous report[2] ranged from 0 to 400 ng/mL. Besides different species, these two studies had two main methodological differences that could account for the discrepancies in reported values: route of administration and dose. The previous study administered 1 mg/kg IV, whereas we used 3 mg/kg IM. Despite the different routes of administration, the fact that we gave three times the dose could easily explain the higher levels we measured in CSF and plasma. In addition, improved LC-MS/MS detection methods and equipment in the 15 plus years since the previous study could have contributed to these differences. We cannot directly compare absolute levels of L-368,899 measured in the brain across these two studies, and many of the regions examined in the two studies differ. But of the three regions that were evaluated in both studies—caudate (striatum), hippocampus, and septum (lateral septum)—the patterns of detected drug are the same: the striatum is at/below the limit of detection, and the lateral septum is the highest, with hippocampus closely behind. We recommend that follow-up studies should also measure AVPR1a and OXTR binding in the same specimens that are analyzed for drug accumulation to provide corresponding protein density measurements to complement drug levels. Because of the nature of the subdissection required to isolate our various regions of interest, we did not preserve the remaining tissue and therefore could not perform quantitative receptor autoradiography to measure actual OXTR or AVPR1a levels in these same specimens.

The binding affinities of L-368,899 that we describe for coyote OXTR and AVPR1a are consistent with those reported for other species (Table 3). L-368,899 binds to coyote OXTR with an affinity of 12.4 nM, which is squarely within the range of binding affinities for rat, macaque, and human OXTR. Although our reported binding affinity for coyote AVPR1a (512 nM) is approximately four to five times lower than that reported for rat, macaque, and human (110 to 180 nM), these values have the same order of magnitude, and our AVPR1a binding affinity was more variable than in other studies. Overall, binding selectivity of L-368,899 appears to be as good as, if not better, in coyotes than in other species, which could more broadly support a general property of this drug as a selective antagonist of mammalian OXTR.

In conclusion, we recommend proceeding with the use of L-368,899 in future behavioral pharmacology studies in coyotes to evaluate the role of the OXTR system in canid social behavior, although additional validation would be useful. Behavioral testing should occur during the 15 to 45 min after injection to align behavioral data collection with the maximal peak of drug in the CNS. When used in vitro, we recommend formulating L-368,899 to a final molarity of 1 to 10 nM to selectively bind coyote OXTR without binding to AVPR1a. Our data set the stage for future use of this compound in coyote behavioral studies.

Acknowledgments

We thank Dr. Arnaud Van Wettere at the Utah Veterinary Diagnostics Lab for technical assistance with brain removals. We also thank Stacey Brummer, Amber Merical, Andalyn Billings, Jeffrey Schultz, and other staff at the Predator Research Facility for their assistance with animal handling.

Funding

This study was funded by the USDA NWRC and by a Research Catalyst seed grant awarded to SMF from the Office of Research at Utah State University. Any use of trade, firm, or product names is for descriptive purposes only and does not imply endorsement by the US government. The findings and conclusions in this publication have not been formally disseminated by the US Department of Agriculture and should not be construed to represent any agency determination or policy.

Conflict of Interest

The authors have no conflicts of interest to declare.

References

1. **Bentler KT, Gossett DN, Root JJ.** 2012. A novel isoflurane anesthesia induction system for raccoons. Wildl Soc Bull **36**:807–812. https://doi.org/10.1002/wsb.193.
2. **Boccia ML, Goursaud A-PS, Bachevalier J, Anderson KD, Pedersen CA.** 2007. Peripherally administered non-peptide oxytocin antagonist, L368,899, accumulates in limbic brain areas: A new pharmacological tool for the study of social motivation in non-human primates. Horm Behav **52**:344–351. https://doi.org/10.1016/j.yhbeh.2007.05.009.
3. **Calcagnoli F, Stubbendorff C, Meyer N, de Boer SF, Althaus M, Koolhaas JM.** 2015. Oxytocin microinjected into the central amygdaloid nuclei exerts anti-aggressive effects in male rats. Neuropharmacology **90**:74–81. https://doi.org/10.1016/j.neuropharm.2014.11.012.
4. **Carlson DA, Gese EM.** 2009. Influence of exogenous gonadotropin-releasing hormone on seasonal reproductive behavior of the coyote (*Canis latrans*). Theriogenology **72**:773–783. https://doi.org/10.1016/j.theriogenology.2009.05.012.
5. **Cavanaugh J, Carp SB, Rock CM, French JA.** 2015. Oxytocin modulates behavioral and physiological responses to a stressor in marmoset monkeys. Psychoneuroendocrino **66**:22–30. https://doi.org/10.1016/j.psyneuen.2015.12.027.
6. **Cavanaugh J, Huffman MC, Harnisch AM, French JA.** 2015. Marmosets treated with oxytocin are more socially attractive to their long-term mate. Front Behav Neurosci **9**:251. https://doi.org/10.3389/fnbeh.2015.00251.
7. **Cavanaugh J, Mustoe AC, Taylor JH, French JA.** 2014. Oxytocin facilitates fidelity in well-established marmoset pairs by reducing sociosexual behavior toward opposite-sex strangers. Psychoneuroendocrinology **49**:1–10. https://doi.org/10.1016/j.psyneuen.2014.06.020.
8. **Cavanaugh J, Mustoe A, French JA.** 2018. Oxytocin regulates reunion affiliation with a pairmate following social separation in marmosets. Am J Primatol **80**:e22750. https://doi.org/10.1002/ajp.22750.
9. **Chiu S-LL, Thompson A, Vincent SH, Alvaro RF, Huskey S-EW, Stearns RA, Pettibone DJ.** 1995. The role of drug metabolism in drug discovery: A case study in the selection of an oxytocin receptor antagonist for development. Toxicol Pathol **23**:124–130. https://doi.org/10.1177/019262339502300204.
10. **Díaz-Muñoz SL, Bales KL.** 2015. "Monogamy" in primates: variability, trends, and synthesis: introduction to special issue on primate monogamy: Primate monogamy. Am J Primatol **78**:283–287. https://doi.org/10.1002/ajp.22463.
11. **Duque-Wilckens N, Steinman MQ, Busnelli M, Chini B, Yokoyama S, Pham M, Laredo SA, et al.** 2017. Oxytocin receptors in the anteromedial bed nucleus of the stria terminalis promote stress-induced social avoidance in female California mice. Biol Psychiatry **83**:203–213. https://doi.org/10.1016/j.biopsych.2017.08.024.
12. **Freeman SM, Young LJ.** 2016. Comparative perspectives on oxytocin and vasopressin receptor research in rodents and primates: Translational implications. J Neuroendocrinol **28**:jne.12382. https://doi.org/10.1111/jne.12382.
13. **Freidinger RM, Pettibone DJ.** 1997. Small molecule ligands for oxytocin and vasopressin receptors. Med Res Rev **17**:1–16. https://doi.org/10.1002/(SICI)1098-1128(199701)17:1<1::AID-MED1>3.0.CO;2-5.
14. **Grippo AJ, McNeal N, Watanasriyakul WT, Cacioppo S, Scotti M-AL, Dagner A.** 2019. Behavioral and cardiovascular consequences of disrupted oxytocin communication in cohabitating pairs of male and female prairie voles. Soc Neurosci **14**:649–662. https://doi.org/10.1080/17470919.2019.1572031.
15. **Harshaw C, Lanzkowsky J, Tran A-QD, Bradley AR, Jaime M.** 2021. Oxytocin and 'social hyperthermia': Interaction with β_3-adrenergic receptor-mediated thermogenesis and significance for the expression of social behavior in male and female mice. Horm Behav **131**:104981. https://doi.org/10.1016/j.yhbeh.2021.104981.
16. **Hennessy CA, Dubach J, Gehrt SD.** 2012. Long-term pair bonding and genetic evidence for monogamy among urban coyotes (*Canis latrans*). J Mammal **93**:732–742. https://doi.org/10.1644/11-MAMM-A-184.1.
17. **Hodges TE, Eltahir AM, Patel S, Bredewold R, Veenema AH, McCormick CM.** 2019. Effects of oxytocin receptor antagonism on social function and corticosterone release after adolescent social instability in male rats. Horm Behav **116**:104579. https://doi.org/10.1016/j.yhbeh.2019.104579.
18. **Huck M, Fiore AD, Fernandez-Duque E.** 2020. Of apples and oranges? The evolution of "monogamy" in non-human primates. Front Ecol Evol **7**:472. https://doi.org/10.3389/fevo.2019.00472.
19. **Kleiman DG.** 1977. Monogamy in mammals. Rev Biol **52**:39–69.
20. **Kotani M, Shimono K, Yoneyama T, Nakako T, Matsumoto K, Ogi Y, Konoike N, Nakamura K, Ikeda K.** 2017. An eye tracking system for monitoring face scanning patterns reveals the enhancing effect of oxytocin on eye contact in common marmosets. Psychoneuroendocrinology **83**:42–48. https://doi.org/10.1016/j.psyneuen.2017.05.009.
21. **Lukas D, Clutton-Brock TH.** 2013. The evolution of social monogamy in mammals. Science **341**:526–530. https://doi.org/10.1126/science.1238677.
22. **Macdonald DW, Campbell LAD, Kamler JF, Marino J, Werhahn G, Sillero-Zubiri C.** 2019. Monogamy: Cause, consequence, or corollary of success in wild canids? Front Ecol Evol **7**:341. https://doi.org/10.3389/fevo.2019.00341.
23. **Mooney SJ, Douglas NR, Holmes MM.** 2014. Peripheral administration of oxytocin increases social affiliation in the naked mole-rat (*Heterocephalus glaber*). Horm Behav **65**:380–385. https://doi.org/10.1016/j.yhbeh.2014.02.003.
24. **Mustoe AC, Cavanaugh J, Harnisch AM, Thompson BE, French JA.** 2015. Do marmosets care to share? Oxytocin treatment reduces prosocial behavior toward strangers. Horm Behav **71**:83–90. https://doi.org/10.1016/j.yhbeh.2015.04.015.
25. **Nowak R, Lévy F, Chaillou E, Cornilleau F, Cognié J, Marnet P-G, Williams PD, Keller M.** 2021. Neonatal suckling, oxytocin, and early infant attachment to the mother. Front Endocrinol (Lausanne) **11**:612651. https://doi.org/10.3389/fendo.2020.612651.
26. **Opie C, Atkinson QD, Dunbar RIM, Shultz S.** 2013. Male infanticide leads to social monogamy in primates. Proc Natl Acad Sci USA **110**:13328–13332. https://doi.org/10.1073/pnas.1307903110.
27. **Pettibone DJ, Clineschmidt BV, Guidotti MT, Lis EV, Reiss DR, Woyden CJ, Bock MG, et al.** 1993. L-368,899, a potent orally active oxytocin antagonist for potential use in preterm labor. Drug Dev Res **30**:129–142. https://doi.org/10.1002/ddr.430300305.
28. **Pettibone DJ, Guidotti M, Harrell CM, Jasper JR, Lis EV, O'Brien JA, Reiss DR, Woyden CJ, Bock MG, Evans BE.** 1995. Progress in the development of oxytocin antagonists for use in preterm labor. Adv Exp Med Biol **395**:601–612.
29. **Shivik JA, Palmer GL, Gese EM, Osthaus B.** 2009. Captive coyotes compared to their counterparts in the wild: Does environmental enrichment help? J Appl Animal Welf Sci **12**:223–235. https://doi.org/10.1080/10888700902955989.
30. **Smith AL, Freeman SM, Barnhart TE, Abbott DH, Ahlers EO, Kukis DL, Bales KL, Goodman MM, Young LJ.** 2016. Initial investigation of three selective and potent small molecule oxytocin receptor PET ligands in New World monkeys. Bioorg Med Chem Lett **26**:3370–3375. https://doi.org/10.1016/j.bmcl.2016.04.097.
31. **Smith AL, Freeman SM, Stehouwer JS, Inoue K, Voll RJ, Young LJ, Goodman MM.** 2012. Synthesis and evaluation of C-11, F-18 and I-125 small molecule radioligands for detecting oxytocin receptors. Bioorg Med Chem **20**:2721–2738. https://doi.org/10.1016/j.bmc.2012.02.019.
32. **Smith AL, Freeman SM, Voll RJ, Young LJ, Goodman MM.** 2013. Carbon-11 N-methyl alkylation of L-368,899 and in vivo PET imaging investigations for neural oxytocin receptors. Bioorg Med Chem Lett **23**:902–906. https://doi.org/10.1016/j.bmcl.2012.10.116.
33. **Smith AL, Freeman SM, Voll RJ, Young LJ, Goodman MM.** 2013. Investigation of an F-18 oxytocin receptor selective ligand via

PET imaging. Bioorg Med Chem Lett **23**:5415–5420. https://doi.org/10.1016/j.bmcl.2013.07.045.

34. **Smith AL, Walum H, Connor-Stroud F, Freeman SM, Inoue K, Parr LA, Goodman MM, Larry JY.** 2017. An evaluation of central penetration from a peripherally administered oxytocin receptor selective antagonist in nonhuman primates. Bioorg Med Chem **25**:305–315. https://doi.org/10.1016/j.bmc.2016.10.035.
35. **Smith AS, Ågmo A, Birnie AK, French JA.** 2010. Manipulation of the oxytocin system alters social behavior and attraction in pair-bonding primates, *Callithrix penicillata*. Horm Behav **57**:255–262. https://doi.org/10.1016/j.yhbeh.2009.12.004.
36. **Takayama K, Tobori S, Andoh C, Kakae M, Hagiwara M, Nagayasu K, Shirakawa H, Ago Y, Kaneko S.** 2022. Autism spectrum disorder model mice induced by prenatal exposure to valproic acid exhibit enhanced empathy-like behavior via oxytocinergic signaling. Biol Pharm Bull **45**:1124–1132. https://doi.org/10.1248/bpb.b22-00200.
37. **Tan O, Musullulu H, Raymond JS, Wilson B, Langguth M, Bowen MT.** 2019. Oxytocin and vasopressin inhibit hyper-aggressive behaviour in socially isolated mice. Neuropharmacology **156**:107573. https://doi.org/10.1016/j.neuropharm.2019.03.016.
38. **Taylor JH, Cavanaugh J, French JA.** 2017. Neonatal oxytocin and vasopressin manipulation alter social behavior during the juvenile period in Mongolian gerbils. Dev Psychobiol **59**:653–657. https://doi.org/10.1002/dev.21533.
39. **Taylor JH, French JA.** 2015. Oxytocin and vasopressin enhance responsiveness to infant stimuli in adult marmosets. Horm Behav **75**:154–159. https://doi.org/10.1016/j.yhbeh.2015.10.002.
40. **Thompson KL, Vincent SH, Miller RR, Colletti AE, Alvaro RF, Wallace MA, Feeney WP, Chiu SH.** 1997. Pharmacokinetics and disposition of the oxytocin receptor antagonist L-368,899 in rats and dogs. Drug Metabolism Dispos **25**:1113–1118.
41. **Tsai T-C, Fang Y-S, Hung Y-C, Hung L-C, Hsu K-S.** 2022. A dorsal CA2 to ventral CA1 circuit contributes to oxytocinergic modulation of long-term social recognition memory. J Biomed Sci **29**:50. https://doi.org/10.1186/s12929-022-00834-x.
42. **Vrachnis N, Malamas FM, Sifakis S, Deligeoroglou E, Iliodromiti Z.** 2011. The oxytocin-oxytocin receptor system and its antagonists as tocolytic agents. Int J Endocrinol **2011**:350546. https://doi.org/10.1155/2011/350546.
43. **Wei D, Lee D, Cox CD, Karsten CA, Peñagarikano O, Geschwind DH, Gall CM, Piomelli D.** 2015. Endocannabinoid signaling mediates oxytocin-driven social reward. Proc Natl Acad Sci USA **112**:14084–14089. https://doi.org/10.1073/pnas.1509795112.
44. **Williams AV, Duque-Wilckens N, Ramos-Maciel S, Campi KL, Bhela SK, Xu CK, Jackson K, Chini B, Pesavento PA, Trainor BC.** 2020. Social approach and social vigilance are differentially regulated by oxytocin receptors in the nucleus accumbens. Neuropsychopharmacology **45**:1423–1430.
45. **Williams PD, Anderson PS, Ball RG, Bock MG, Carroll L, Chiu SH, Clineschmidt BV, Culberson JC, Erb JM, Evans BE.** 1994. 1-(((7,7-Dimethyl-2(S)-(2(S)-amino-4-(methylsulfonyl)butyramido) bicyclo[2.2.1]heptan-1(S)-yl)methyl)sulfonyl)-4-(2-methylphenyl) piperazine (L-368,899): An orally bioavailable, non-peptide oxytocin antagonist with potential utility for managing preterm labor. J Med Chem **37**:565–571. https://doi.org/10.1021/jm00031a004.